

Tomoya Matsutomi · Chizumi Nakamoto · Taixing Zheng · Jun-ichi Kakimura ·
Nobukuni Ogata

**Multiple types of Na⁺ currents mediate action potential
electrogenesis in small neurons of mouse dorsal root
ganglia**

Tomoya Matsutomi · Chizumi Nakamoto · Zheng Taixing · Jun-ichi Kakimura ·
Nobukuni Ogata (✉)

Department of Neurophysiology, Graduate School of Biomedical Sciences,
Hiroshima University, Hiroshima, 734-8551, Japan

e-mail: ogatan@hiroshima-u.ac.jp

Tel.: +81-82-257-5125, Fax: +81-82-257-5125

Abstract Small ($< 25 \mu\text{m}$ in diameter) neurons of the dorsal root ganglion (DRG) express multiple voltage-gated Na^+ channel subtypes, 2 of which being resistant to tetrodotoxin (TTX). Each subtype mediates Na^+ current with distinct kinetic property. However, it is not known how each type of Na^+ channels contributes to the generation of action potentials in small DRG neurons. Therefore, we investigated the correlation between Na^+ currents in voltage-clamp recordings and corresponding action potentials in current-clamp recordings, using wild-type (WT) and $\text{Na}_v1.8$ knock-out (KO) mice, to clarify action potential electrogenesis in small DRG neurons. We classified Na^+ currents in small DRG neurons into three categories on the basis of TTX sensitivity and kinetic properties i.e., TTX-sensitive (TTX-S)/fast Na^+ current, TTX-resistant (TTX-R)/slow Na^+ current and TTX-R/persistent Na^+ current. Our concurrent voltage-clamp and current-clamp recordings from the same neuron revealed that action potentials in WT small DRG neurons were mainly dependent on TTX-R/slow Na^+ current mediated by $\text{Na}_v1.8$. Surprisingly, a large portion of TTX-S/fast Na^+ current was switched off in WT small DRG neurons due to a hyperpolarizing shift of the steady-state inactivation (h_∞), whereas in KO small DRG neurons which are devoid of TTX-R/slow Na^+ current, action potentials were generated by TTX-S/fast Na^+ current possibly through a compensatory shift of h_∞ in the positive direction. We also confirmed that TTX-R/persistent Na^+ current mediated by $\text{Na}_v1.9$ actually regulate subthreshold excitability in small DRG neurons. In addition, we demonstrated that TTX-R/persistent Na^+ current can carry an action potential when the amplitude of this current was abnormally increased. Thus, our results indicate that the action potentials in small DRG neurons are generated and regulated with a combination of multiple mechanisms that may give rise to unique functional properties of small

DRG neurons.

Keywords

Na⁺ channel · Dorsal root ganglion · Tetrodotoxin · Patch clamp · Action potential · Gating · Pain

Introduction

Primary sensory neurons transmit a broad range of sensory information from the periphery to the spinal cord. They are highly differentiated morphologically as well as functionally, and each type of them mediates different modalities of sensation. Unmyelinated C fibers or thinly myelinated A δ fibers, which originate from smaller types of dorsal root ganglion (DRG) neurons, mainly mediate nociceptive information, whereas myelinated A β fibers, which originate from larger types of DRG neurons, are thought to largely mediate innocuous information. Voltage-gated Na⁺ channels play critical roles in the conduction of sensory information in DRG neurons, because they are responsible for the upstroke of conducting action potentials.

To date, nine isoforms of Na⁺ channel α -subunits have been cloned from mammals, and at least seven among them are identified in DRG neurons [18]. While Na⁺ channel α -subunits sensitive to tetrodotoxin (TTX), including Na_v1.1, Na_v1.2, Na_v1.6 and Na_v1.7, are widespread in all types of DRG neurons [4], TTX-resistant (TTX-R) Na⁺ channel α -subunits (Na_v1.8 and Na_v1.9) are preferentially expressed in small DRG neurons, suggesting their important roles in nociception [1,15,16].

The preferential expression of TTX-R Na⁺ channel α -subunits in small DRG neurons might result in the generation of action potentials with distinct functional properties that are probably involved in the segregation of sensory modalities. However, it has not been determined how each type of Na⁺ channels contributes to the generation and propagation of action potentials in small DRG neurons. In this study, therefore, we investigated the correlation between Na⁺ current in voltage-clamp recording and action potential in current-clamp recording using wild-type (WT) and Na_v1.8 knock-out (KO) mice to clarify action potential electrogenesis in small DRG neurons.

Materials and methods

Isolation of single DRG neurons and cell culture

Breeding pairs of Nav1.8 heterozygous mice [2] were generously provided by Prof. John Wood. A colony of WT and KO mice were raised from these pairs, and KO mice were compared with littermate WT mice. All procedures were carried out according to protocols approved by Hiroshima University Animal Ethics Committee. Adult mice were sacrificed by cervical dislocation during ethylcarbamate (3 mg/g) anaesthesia. The DRGs from all spinal levels were removed and desheathed in ice-cold, Ca²⁺/Mg²⁺-free, phosphate-buffered saline. The isolated DRGs were enzymatically digested at first with 0.2 % collagenase (Wako, Osaka, Japan) and then with 0.1 % trypsin (Sigma, St. Louis, Mo., USA), each for 20 min at 37 °C. The DRGs were then dissociated by trituration with fire-polished Pasteur pipettes, and cells were plated onto glass coverslips coated with 0.01 % poly-L-lysine (Sigma).

The dispersed DRG neurons were maintained in a humidified incubator containing 5 % CO₂ in air at 36 °C in Dulbecco's modified Eagle medium supplemented with 10 % heat inactivated fetal bovine serum (Gibco, Grand Island, NY., USA), penicillin (100 IU/ml) and streptomycin (100 µg/ml). Cells under short-term culture (4 to 12 hr after plating) were used for experiments. At this time in culture, neurite outgrowth was not observed. We defined DRG neurons that were smaller than 25 µm in diameter as small neurons [3], and small neurons thus defined were used throughout the study. Since KO DRG neurons [2,25] express only Nav1.9, the properties of Nav1.9-mediated Na⁺ current can be studied in

isolation. Therefore, we employed KO DRGs in addition to WT DRGs in this study. Unless otherwise specified, the experiments were made in neurons from WT DRGs.

Electrophysiology

Voltage-clamp recordings were performed using an Axopatch 200A amplifier (Axon Instruments, Union City, Calif., USA). Data were low-pass-filtered at 5 kHz with a four-pole Bessel filter and digitally sampled at 25-100 kHz. In some experiments, capacitive and leakage currents were subtracted digitally by the P-P/4 procedure [27]. Membrane currents were recorded using the whole-cell patch-clamp technique. The patch pipette solution contained (in mM): 10 NaCl, 110 CsCl, 20 tetraethylammonium (TEA)-Cl, 2.5 MgCl₂, 5 HEPES and 5 EGTA. The pH of the pipette solution was adjusted to 7.0 with CsOH. Osmolarity was adjusted to 290 mosmol/kg with glucose. The DC resistance of patch electrodes was 0.8–1.5 MΩ.

The bath solution contained (in mM): 100 NaCl, 5 CsCl, 30 TEA-Cl, 1.8 CaCl₂, 1 MgCl₂, 0.1 CdCl₂, 5 HEPES, 25 glucose and 5 4-aminopyridine (4-AP). TEA-Cl and 4-AP were added to abolish K⁺ currents and Cd²⁺ was added to abolish Ca²⁺ currents [27]. The pH of the bath solution was adjusted to 7.4 with HCl (since 4-AP is strongly alkalic). Osmolarity was adjusted to 290 mosmol/kg with glucose. The liquid junction potential between internal and external solutions was compensated for by adjusting the zero current potential to the liquid junction potential. Only cells showing an adequate voltage- and space-clamp [27] were used. Most recordings from small DRG neurons could be performed without voltage- and space-clamp problems owing to their small size and round cell bodies

that were devoid of apparent processes. Recordings, in which Na⁺ current activation was not gradual with incrementing depolarization showing an obvious threshold phenomenon, were excluded from the analysis.

Current-clamp recordings were performed by switching to current-clamp mode after a stable whole-cell configuration was formed in voltage-clamp mode. The patch pipette solution contained (in mM): 10 NaCl, 130 KCl, 2.5 MgCl₂, 5 HEPES and 5 EGTA. The pH of the pipette solution was adjusted to 7.0 with KOH. Osmolarity was adjusted to 290 mosmol/kg with glucose. In some experiments, total KCl was replaced with an equimolar amount of KF. The DC resistance of patch electrodes was 0.8–1.5 MΩ. The bath solution contained (in mM): 130 NaCl, 5 KCl, 1.8 CaCl₂, 1 MgCl₂, 0.1 CdCl₂, 5 HEPES and 25 glucose. The pH of the bath solution was adjusted to 7.4 with NaOH. Osmolarity was adjusted to 290 mosmol/kg with glucose. These internal and external solutions were also used in experiments where voltage-clamp recordings were performed in addition to current-clamp recordings in the same DRG neuron.

The membrane potential was adjusted to the desired potential level by means of DC current injection through a recording patch electrode. The current intensity required to evoke an action potential was determined by a series of depolarizing currents from 10 pA up to 250 pA in 10-pA step increments. The voltage threshold for action potential generation was measured at the beginning of the sharp upward rise of the depolarizing phase of action potential.

Experiments were performed at room temperature (21–23 °C). Data were expressed as means ± S.E.M., and *n* represents the number of cells examined. Statistical Significance was evaluated using Student's t-test or the Mann-Whitney U test. *P* < 0.01 was considered significant.

Results

Characterization of Na⁺ currents in small DRG neurons

It has been shown by many investigators that three distinct categories of Na⁺ currents have been classified in small DRG neurons, on the basis of TTX sensitivity and kinetic properties [3,12,20,25,31]. One type of Na⁺ current is a transient type of TTX-sensitive (TTX-S) Na⁺ current, which rapidly activates and inactivates. In this paper, we call this Na⁺ current "TTX-S/fast Na⁺ current". The remaining two are the TTX-resistant (TTX-R) Na⁺ currents mediated by Nav1.8 and Nav1.9. Since TTX-R Na⁺ current mediated by Nav1.8 activates and inactivates more slowly than TTX-S/fast Na⁺ current [1,27,34], we call it "TTX-R/slow Na⁺ current". TTX-R Na⁺ current mediated by Nav1.9 is characterized by an extremely prolonged time course at low activation voltages [12,14,25]. From its pharmacological and kinetic properties, we call this Na⁺ current "TTX-R/persistent Na⁺ current".

Although the kinetic properties of these Na⁺ currents have already been shown in a number of reports, it appears that the actual values of the kinetic parameters are not consistent possibly due to different experimental conditions, e.g., distinctive ionic compositions of the internal and external solutions or different pulse protocols employed to measure kinetic parameters [1,3,12,14,25,27,31]. In addition, it has not been possible to reliably separate TTX-R Na⁺ currents until kinetic properties of Na⁺ current mediated by Nav1.9 have been disclosed [3,12,14,20,25,31]. Therefore, we tried to measure some of the fundamental kinetic parameters under the same experimental condition.

Na⁺ currents were recorded in small DRG neurons from WT and KO [2,25] mice. TTX-S/fast Na⁺ current was isolated by subtracting the current remaining after

application of 200 nM TTX from the total Na⁺ current in both WT and KO neurons. Since TTX-R/persistent Na⁺ current has an activation threshold about 20 mV more negative than the threshold for TTX-R/slow Na⁺ current [25], it was possible to check whether or not the cell under voltage-clamp recording has a TTX-R/persistent Na⁺ current. TTX-R/slow Na⁺ current could be obtained from WT neurons that were devoid of TTX-R/persistent Na⁺ current. TTX-R/persistent Na⁺ current was obtained from KO neurons in the presence of 200 nM TTX. To measure the activation threshold for each Na⁺ current, the holding potential (V_H) was set to -80 mV and the command potential was successively increased in 2 mV step from an initial value of -50 mV (for TTX-S/fast Na⁺ current and TTX-R/slow Na⁺ current) or -70 mV (for TTX-R/persistent Na⁺ current) until a detectable Na⁺ current could be elicited.

Measurements of ion channel kinetics such as the current-voltage (I-V) relationship or the steady-state inactivation (h_∞) generally take a considerable time to execute the protocol, since a sufficient recovery period for the channel must be allowed between each test pulse (V_T). The amplitudes of Na⁺ currents are not always constant during recording, e.g. due to run-down of the current or to instability of the seal condition. This can be checked by applying a control pulse (V_C) prior to each V_T . To avoid a possible time-dependent distortion of the analysis, V_C to a fixed voltage was applied 15 s prior to V_T (for measurement of I-V relationship) or the conditioning prepulse (for measurement of h_∞). The amplitude of the current evoked by V_C (I_C) served as a gatekeeper for the stability of the current. This method was also useful in removing a possible involvement of extremely slow inactivation process. Measurements in which the amplitude of I_C showed a change exceeding 20% were discarded. In addition, the amplitude of the

current evoked by V_T (I_T) was expressed as I_T/I_C .

Typical examples of the above three categories of Na^+ currents are shown in Fig. 1 together with respective I-V curves and m_∞ curves. TTX-S/fast Na^+ current could be observed in most of the neurons recorded irrespective of their genomic type (60/63 in WT neurons and 57/57 in KO neurons). TTX-S/fast Na^+ current had an activation threshold at -42 mV in both WT and KO neurons. TTX-R/slow Na^+ current could be observed in 54 out of 63 WT neurons and totally absent in KO neurons [25]. TTX-R/slow Na^+ current was activated at -40 mV, which was not significantly different from the threshold for TTX-S/fast Na^+ current. TTX-R/persistent Na^+ current could be observed in 39 out of 63 WT neurons and 37 out of 57 KO neurons. The threshold for TTX-R/persistent Na^+ current was -61 mV in both WT and KO neurons, much more negative than the thresholds for TTX-S/fast Na^+ current and TTX-R/slow Na^+ current. Statistical data are shown in Table 1. The m_∞ curve was measured according to the method described by Ogata & Tatebayashi [27]. Since most of the WT neurons that expressed TTX-R/persistent Na^+ current also expressed TTX-R/slow Na^+ current, it was practically impossible to measure the m_∞ curve for TTX-R/persistent Na^+ current in WT neurons. The voltage for half-maximal activation ($V_{1/2}$ of activation) and the slope factor are summarized in Table 1.

Comparison of the steady-state inactivation curves

The duration of the conditioning prepulse (V_{PRE}) strongly affects the characteristics of h_∞ parameters. For example, h_∞ curves for TTX-R Na^+ current was shifted in

more depolarizing direction when the duration of V_{PRE} was set to shorter duration [26]. Therefore, the same pulse protocol should be applied to compare the inactivation characteristics of different Na^+ currents. In this study, we used the h_{∞} parameter as an estimate of "channel availability at the resting membrane potential". Thus, the duration of V_{PRE} was the longer the better, since the longer V_{PRE} leads Na^+ channel availability to steady-state at V_{PRE} , whereas the longer V_{PRE} prolongs total duration of the pulse protocol for measurement of h_{∞} . Balancing the merits and demerits, the duration of V_{PRE} was set to 3 s for all three categories of Na^+ current.

Fig. 2 illustrates h_{∞} curves of different types of Na^+ current and their Boltzmann parameters are summarized in Table 1. It was possible to measure h_{∞} for TTX-R/persistent Na^+ current in WT neurons, since the inactivation time course of this current was extremely prolonged as compared with that of TTX-R/slow Na^+ current. Surprisingly, the h_{∞} curve for TTX-S/fast Na^+ current in KO neurons was more depolarized than that in WT neurons. The h_{∞} curve for WT small DRG neurons (open circles) had $V_{1/2}$ of -93.2 mV. The value of h_{∞} became 0 at potentials positive to about -70 mV. On the contrary, the h_{∞} curve for KO DRG neurons (filled circles) had $V_{1/2}$ of -73.3 mV, which was about 20 mV more positive than the value for WT DRG neurons. $V_{1/2}$ of the h_{∞} curve for TTX-R/slow Na^+ current (triangles) was more positive than the values obtained for TTX-S/fast Na^+ current.

A good voltage-clamp control was required for measurement of the h_{∞} curve of TTX-R/persistent Na^+ current, due to unusual properties of this current. Since the h_{∞} curve for TTX-R/persistent Na^+ current overlaps with the m_{∞} curve in a wide voltage range [25], a considerable amount of inward current flows persistently at voltages where h_{∞} is not zero. When the membrane voltage is not satisfactory

clamped, this persistent current produces an erroneous deviation of the actual membrane potential from V_T , thus causing a negative shift of the h_∞ curve at voltages positive to the threshold for TTX-R/persistent Na^+ current (-60 mV). There was no significant difference in $V_{1/2}$ of the h_∞ curve for TTX-R persistent Na^+ current between WT and KO neurons. This parameter in both WT and KO neurons measured using our experimental protocol was about 10 mV more positive than that for TTX-R/slow Na^+ current. The values of $V_{1/2}$ for TTX-R/slow Na^+ current and TTX-R/persistent Na^+ current were more hyperpolarized than those reported by other investigators (e.g., [12, 17]). This discrepancy may be due to an extremely longer V_{PRE} (3 s) employed in our study.

Functional relationships between Na^+ currents and action potential generation in small DRG neurons

To investigate relationships between Na^+ currents and action potential generation in small DRG neurons, we performed combined recordings of voltage-clamp and current-clamp modes in the same neuron. The membrane potential was held to a desired level by applying inward or outward DC current injection in current-clamp mode. Since the resting membrane potential of small DRG neurons measured in current-clamp recording was -58.1 ± 2.6 mV for WT mice and -60.2 ± 2.8 mV for KO mice ($n = 25$, respectively) in our experiments, we at first set V_H in voltage-clamp mode and the membrane potential in current-clamp mode to -60 mV.

In the voltage-clamp mode (Fig. 3A), Na^+ current was evoked in the small WT DRG neuron by V_T to 0 mV. The Na^+ current had slow activation and inactivation

time courses and was not affected by 200 nM TTX. Then, the recording was switched to the current-clamp mode in the same neuron (Fig. 3B). An action potential was evoked by a depolarizing current injection of 80 ms in duration from a membrane potential of -60 mV. TTX in a concentration of 200 nM had no detectable effect on the action potential generation.

We switched back to the voltage-clamp mode and V_H was changed to -100 mV from -60 mV (Fig. 3C). In the recordings of a negative V_H of -100 mV, the activation time course of Na^+ current was accelerated although the time to peak of the current did not appreciably change. In addition, the peak amplitude was increased. An increased outward current may be due to an increased transient type of K^+ current that was brought about by a negative shift of V_H . Na^+ currents observed at V_H of -100 mV were partially blocked by 200 nM TTX (Fig. 3D), indicating that TTX-S Na^+ current was involved in the action potential electrogenesis.

Again in the current-clamp mode, an action potential was evoked from a membrane potential of -100 mV (Fig. 3E). The peak amplitude of the action potential recorded at a membrane potential of -100 mV was partially blocked by 200 nM TTX. Similar results were obtained in all of the 9 cells examined. The pooled data showed that the current intensity for an action potential generation was 86.0 ± 2.2 pA ($n = 9$) at a membrane potential of -60 mV and 185.6 ± 4.7 pA ($n = 9$) at -100 mV, whereas the threshold for action potential generation was not significantly different (-40.2 ± 0.5 mV for -60 mV and -41.2 ± 0.4 mV for -100 mV, $n = 9$, respectively).

As shown in Fig. 3F, repetitive firing of action potentials could be recorded in small WT neurons during a longer depolarizing current injection in the presence of

200 nM TTX, irrespective of membrane potential. Such a repetitive firing was observed in 8 cells out of 20 cells examined.

In small neurons of KO DRGs, Na⁺ currents that activate and inactivate rapidly were evoked by V_T to 0 mV from V_H of -80 mV in the voltage-clamp mode (Fig. 4A). This Na⁺ current was completely abolished by 200 nM TTX. In the current-clamp mode, an action potential was evoked from a membrane potential of -60 mV (Fig. 4B). The current intensity required to evoke an action potential generation was 82.0 ± 2.0 pA ($n = 10$) and the threshold for action potential generation of -41.6 ± 0.5 mV ($n = 10$). When 200 nM TTX was applied, the depolarizing current injection failed to elicit an action potential in all of the 6 cells tested (Fig. 4B). Repetitive firing of action potential was not observed in any of the 6 cells tested even when the intensity and duration of the depolarizing current injection were increased.

Sustained effects of TTX-R/persistent Na⁺ current on action potential generation in small DRG neurons

In small DRG neurons, the current-clamp recordings were performed from a membrane potential of -80 mV. Membrane potential changes evoked by 30 ms successive depolarizing current injections (10 - 60 pA, in 10 pA step increase) were recorded and shown superimposed in WT (Fig. 5A) and KO (Fig. 5B) neurons. At weak depolarizing current intensities (10 - 30 pA), membrane potential changes mainly reflected a passive electrotonic response. When the intensity of the current injection was increased to 40 pA, the apparently active membrane response was

observed during and after the depolarizing current injection adding to the passive electrotonic response (open arrows).

On further increasing the intensity of the current injection to 50 pA, a much larger active membrane response was evoked and continued to develop forming a sustained membrane depolarization even after the depolarizing current injection (closed arrows) and eventually elicited an action potential (dots). The latency of action potential generation from the onset of the depolarizing current injection was shortened by further increasing the current intensity to 60 pA (triangles).

The sustained membrane depolarization was not a depolarizing afterpotential (DAP) following an action potential, since this depolarization could be evoked at subthreshold potentials independently of action potential generation (see Fig. 5A and B, open arrows). The sustained membrane depolarization remained unaffected by TTX in both WT (Fig. 5C) and KO (Fig. 5D) neurons, whereas an action potential was abolished by 200 nM TTX in KO neurons (D) but not in WT neurons (C). The sustained membrane depolarization was observed in 61.5 % (16/26) of WT neurons and 67.9 % (19/28) of KO neurons. Since the threshold for the sustained membrane depolarization was found at around -60 mV in our preliminary experiments, it was necessary to set the membrane potential to potentials more negative than -60 mV to precisely determine the threshold for the sustained membrane depolarization. The current intensity to trigger the sustained membrane depolarization was 34.2 ± 1.9 pA ($n = 12$) for WT neurons and 33.6 ± 2.0 pA ($n = 11$) for KO neurons. The threshold for the sustained membrane depolarization was -60.8 ± 0.6 mV ($n = 12$) for WT neurons and -61.1 ± 0.6 mV ($n = 11$) for KO neurons. There was no significant difference in these parameters between WT and KO neurons.

The intensity of the current injection to evoke an action potential and the action potential threshold in small DRG neurons with or without sustained membrane depolarization were summarized in Table 2. In both WT and KO neurons, the current intensity required to evoke an action potential was significantly smaller in neurons where the sustained membrane depolarization was observed than in neurons that were devoid of sustained membrane depolarization. However, the threshold for action potential generation was not significantly different between the two groups of neurons, regardless of the presence or absence of the sustained membrane depolarization. The above two parameters showed similar values in WT and KO neurons.

To estimate the duration of the sustained membrane depolarization, the total duration of the trace was extended to 500 ms in the same neurons as those shown in Fig. 5. The sustained membrane depolarization was evoked by a depolarizing current injection in a duration of 50 ms from a membrane potential of -80 mV (Fig. 6). The sustained membrane depolarization lasted even after the end of the depolarizing current injection in both WT (A) and KO (B) neurons. The mean duration of the sustained membrane depolarization was 307 ± 34 ms ($n = 5$) for WT neurons and 302 ± 41 ms ($n = 5$) for KO neurons, respectively. There was no significant difference between these two values.

The above results suggest that the sustained membrane depolarization was probably evoked by TTX-R/persistent Na^+ current. Nevertheless, the persistent component of Na^+ current was not apparent in the concurrent voltage-clamp recordings (Fig. 7A1 and B1). In the bath solution employed for current-clamp recording in which K^+ channel blockers were not included, the large outward current followed the inward current in both WT (A1) and KO (B1) neurons. In these cases,

persistent Na^+ current could be cancelled by the large outward K^+ current. For this reason, K^+ channel blockers (30 mM TEA and 5 mM 4-AP) were added under the voltage-clamp mode. As shown in Fig. 7A2 and B2, an application of the bath solution containing K^+ channel blockers abolished the large portion of the outward current, and the persistent inward component was disclosed in either WT (A2) or KO (B2) neurons.

It should be noted that the initial component of the inward current in WT neurons (Fig. 7A2) had slower activation and inactivation time courses as compared to those in KO neurons (Fig. 7B2). On applying 200 nM TTX, the initial component of the inward current in WT neurons remained largely unaffected (Fig. 7A3) whereas that in KO neurons was completely abolished (Fig. 7B3). On the contrary, the persistent inward component was not affected by TTX in either WT (Fig. 7A3) or KO neurons (Fig. 7B3). The persistent inward current was detectable only in neurons that showed the sustained membrane depolarization in the preceding current-clamp mode.

Effects of augmented TTX-R/persistent Na^+ current on action potential generation in small DRG neurons

We previously reported that the peak amplitude of TTX-R/persistent Na^+ current recorded with F^- as an internal anion was generally much larger than that recorded with Cl^- in voltage-clamp recordings [25]. In addition, kinetic properties of TTX-R/persistent Na^+ current were markedly affected by internal F^- [12,25]. Therefore, findings obtained in the presence of internal F^- may not be relevant to

physiological significance of TTX-R/persistent Na^+ current. Nevertheless, to examine the effect of augmented TTX-R/persistent Na^+ current on action potential generation may afford us some important implication regarding action potential electrogenesis in small DRG neurons.

We replaced KCl in the patch pipette solution with an equimolar amount of KF. Since the h_∞ curve for TTX-R/persistent Na^+ current is extremely shifted in the negative direction when F^- is used as an internal anion [12,25,31], an appreciable amount of TTX-R/persistent Na^+ current could not be obtained at V_H of -80 mV [25]. For this reason, the recordings were performed from a negative membrane potential of -100 mV.

In small neurons from KO DRGs, membrane potential changes evoked by depolarizing current injections in 10 pA step increase were recorded and shown superimposed in Fig. 8A. As has been shown in Fig. 5, weak depolarizing current injections evoked a passive electrotonic response, while an apparently active membrane response accompanying an all-or-none action potential generation was triggered on increasing the intensity of the current injection. The latency of action potential generation was successively shortened by further increasing the current intensity. When 200 nM TTX was applied, the action potential was abolished and, instead, a small depolarization was disclosed (Fig. 8B).

Unlike the observation in the absence of 200 nM TTX (Fig. 8A), the small depolarization grew up gradually depending on the intensity of the depolarizing current injection, and finally developed into a full-blown action potential (Fig. 8C). Namely, the action potential evoked in the presence of TTX did not occur in an all-or-none manner. It should be noted that such an action potential in the presence of TTX was not observed with Cl^- as an internal anion in KO neurons (see

Fig. 5D). The latency of the action potential or the small depolarization was successively shortened when the current intensity was increased.

Discussion

h_{∞} curves in small DRG neurons

In the present study, we confirmed the heterogeneous expression of multiple types of Na^+ currents with different kinetic properties in small neurons of mouse DRG. The resting membrane potential of DRG neurons has been studied by many investigators in the mouse [7,19,21,43] and rat [13,14,36]. The resting membrane potential of mouse small DRG neurons was found most typically in a voltage range of -70 to -50 mV, and the data obtained in the present study (about -60 mV in both WT and KO neurons) were within this voltage range.

Surprisingly, h_{∞} values for TTX-S/fast Na^+ current in WT neurons were substantially zero at this potential range (Fig. 2, open circles). Such an extremely negative h_{∞} has already been reported in rat small DRG neurons [27]. It appears that the negative h_{∞} is a property inherent in small DRG neurons, since the negative h_{∞} has not been found in either the rat large DRG neurons [27] or the mouse large DRG neurons larger than 30 μm in diameter (unpublished observation). Due to this striking difference in h_{∞} values noted between TTX-S and TTX-R Na^+ currents, the h_{∞} curve in small DRG neurons was characterized by a prominent two components (see Fig. 10 in [27]). Thus, it may be suggested that a large portion of the Na^+ channels which mediates TTX-S/fast Na^+ current in WT small DRG neurons may not function at resting membrane potential due to inactivation. On the contrary, since the $V_{1/2}$ value for TTX-R/slow Na^+ current was found at the potential more positive to resting membrane potential (Fig. 2, triangles), this current is thought to be available at resting membrane potential in WT small DRG neurons.

The h_{∞} curve for TTX-S/fast Na^+ current was modulated in the deletion mutant

of TTX-R/slow Na⁺ current (Fig. 2, filled circles). The positive shift of h_{∞} indicates that a considerable number of Na⁺ channels that mediate TTX-S/fast Na⁺ current remain available at resting membrane potential in KO neurons. There may be several possibilities to explain the above difference found for WT and KO DRG neurons. The one possibility is that the distinct class of Na⁺ channels mediating TTX-S/fast Na⁺ current that has positive h_{∞} was newly upregulated in KO neurons. Another possibility might be that the inactivation kinetics of the TTX-S/fast Na⁺ current has been modulated in mutant neurons.

At present, we can not rule out either possibility to explain the distinctive property of the h_{∞} curve noted for KO neurons. The former possibility is not unlikely in view of the findings that Nav1.7 transcript and TTX-S Na⁺ current were actually upregulated in the deletion mutant of TTX-R/slow Na⁺ current [2] and that Nav1.3 transcript or immunoreactivity was dramatically upregulated after nerve injury [5,24,41]. On the contrary, our observation that the h_{∞} curve for TTX-S/fast Na⁺ current in KO neurons was well described by a single Boltzmann function with the slope factor comparable to that obtained from WT neurons may be in favor of the latter possibility. If an additional Na⁺ channel subtype was upregulated in KO neurons, the h_{∞} curve should consist of two components. Moreover, other kinetic properties of TTX-S/fast Na⁺ current observed in KO neurons were very similar to those observed in WT neurons (Table 1). Therefore, it is possible that the shift of the h_{∞} curve for TTX-S/fast Na⁺ current found for KO neurons may be brought about by a compensatory mechanism as a result of deletion of Nav1.8, rather than expression of new type of TTX-S Na⁺ channel.

Several hypotheses have been reported for the mechanism underlying the shift of the h_{∞} curve for Na⁺ channels, including phosphorylation of Na⁺ channels by

protein kinase C (PKC) or protein kinase A (PKA) [9,10,39], regulation through β -subunits [29,40] and modulation by endogenous substances such as arachidonic acid [23]. It is unknown for the moment regarding the mechanism by which the shift of the h_{∞} curve for TTX-S/fast Na^+ current is brought about, and further study is required to clarify the mechanism underlying the shift of h_{∞} .

Action potential electrogenesis

The above discussion based on the h_{∞} curve was potentially useful together with our combined voltage-clamp and current-clamp recordings for understanding of the action potential electrogenesis in small DRG neurons. In WT small DRG neurons, TTX-R/slow Na^+ current appears to play a principal role in the generation of action potential evoked by a depolarizing current injection from resting membrane potential, because the action potential evoked from a membrane potential of -60 mV was not affected by an application of TTX (Fig. 3B). This finding further indicates that the TTX-R action potentials play an important role in the soma of small DRG neurons [30] as well as in nerve endings of sensory neurons that innervate the intracranial dura mater [38] or the cornea [6].

In recordings from a negative membrane potential (-100 mV), we found that TTX-S/fast Na^+ current may be involved in the generation of action potential, since the action potential was partially blocked by TTX (Fig. 3E). This observation might indicate that TTX-S/fast Na^+ current, which is inactivated at resting membrane potential, may also play a part in action potential generation when the membrane is excessively hyperpolarized in pathological condition. It should be

noted that, in KO neurons, an action potential generation was dependent on TTX-S/fast Na⁺ current probably due to the absence of Na_v1.8 that normally carries an action potential generation in WT neurons (Fig. 4B). This observation is in agreement with the result obtained in the voltage-clamp recording that a considerable fraction of Na⁺ channels mediating TTX-S/fast Na⁺ current could function at resting membrane potential in KO neurons (see the h_{∞} curve for TTX-S/fast Na⁺ current of KO neurons in Fig. 2).

Repetitive firing is observed in WT neurons where TTX-R/slow Na⁺ current probably mediated the generation of action potential (Fig. 3F), but not in KO neurons where TTX-S/fast Na⁺ current probably mediated the action potential. This finding supports the notion proposed by Elliot and Elliot [17] that the TTX-R/slow Na⁺ current is involved in repetitive firing of DRG neurons. The repetitive firing in small neurons from WT DRGs may be related to the fact that TTX-R/slow Na⁺ current recovers from inactivation more rapidly than TTX-S/fast Na⁺ current when the duration of the depolarizing pulse applied to inactivate Na⁺ channels is relatively short (20 ms [13], 40 ms [35] and 60 ms [17,33]), probably due to the lack of slow inactivation of TTX-R/slow Na⁺ current [26]. Since the action potential is a short event which usually lasts for several milliseconds, TTX-R/slow Na⁺ current may rapidly recover from fast inactivation during depolarizing current injection and may cause repetitive firing in small neurons from WT DRGs.

Regulation of action potential generation by persistent Na⁺ currents

In small neurons from WT DRGs, both the action potential and the subthreshold sustained membrane depolarization were not affected by TTX (Fig. 5C), indicating that TTX-R Na⁺ channels mediate these electrical events. On the contrary, only the action potential was blocked by TTX in small neurons from KO DRGs (Fig. 5D). These results further strengthen the possibility that the upstroke of action potential is carried by TTX-R/slow Na⁺ current in WT neurons and by TTX-S/fast Na⁺ current in KO neurons.

The sustained membrane depolarization observed in both WT and KO neurons was resistant to TTX. In addition, in voltage-clamp recordings from neurons that revealed the sustained membrane depolarization (Fig. 7), an application of K⁺ channel blockers disclosed the TTX-R persistent inward component (A2 and B2), which has been masked by the concurrent large outward component. These results indicate that the sustained membrane depolarization is associated with TTX-R/persistent Na⁺ current mediated by Na_v1.9. It has been shown that the peak amplitude of TTX-R/persistent Na⁺ current increases dramatically during whole-cell recordings, as if inactive or silent channels have been ‘kindled’ [3,25]. Therefore, there is a possibility that the sustained membrane depolarization by TTX-R/persistent Na⁺ current may be evoked by such an unusual upregulation of TTX-R/persistent Na⁺ current.

A similar sustained membrane depolarization mediated by Na_v1.9 described by Coste *et al.* lasted for several seconds (see Fig. 6C of [12]), whereas the sustained membrane depolarization in our study lasted for at most several hundreds milliseconds (Fig. 6). Coste *et al.* used F⁻ as an internal anion in their recording [12], whereas we used Cl⁻. Since the peak amplitude of TTX-R/persistent Na⁺ current recorded with F⁻ is abnormally up-regulated in voltage-clamp recordings

[25], the up-regulation of TTX-R/persistent Na⁺ current by F⁻ might have caused the conspicuous prolongation of the sustained membrane depolarization. In addition, Coste *et al.* used the internal and external solutions containing Cs⁺ ions that block K⁺ channels [12], whereas K⁺ channel blockers were not used in our recordings. Thus, the blocking of K⁺ currents may also be responsible for the prolongation of the sustained membrane depolarization.

The threshold for the sustained membrane depolarization was more negative than the threshold for action potential generation, in agreement with the finding in the voltage-clamp recording that the activation threshold for TTX-R/persistent Na⁺ current was more negative than the activation thresholds for Na⁺ currents that mediate action potential generation, i.e., TTX-S/fast Na⁺ current and TTX-R/slow Na⁺ current (Table 1). Action potentials were evoked with smaller current intensity in neurons where the sustained membrane depolarization was observed than in neurons which lacked the sustained membrane depolarization (Table 2).

In addition, the sustained membrane depolarization that continued to develop even after the depolarizing current injection could eventually induce action potential generation (Figs. 5 and 6). These results confirm that the sustained membrane depolarization evoked by TTX-R/persistent Na⁺ current exerts facilitatory effects on action potential generation [14,20]. Since the sustained membrane depolarization outlasted for more than several hundreds milliseconds even in the absence of K⁺ channel blockers, this depolarization may also contribute to setting both resting membrane potential and subthreshold electrogenesis as has been suggested by a computer simulation [20]. Such a regulation of the membrane potential by TTX-R/persistent Na⁺ current may give a remarkable effect on the excitability of small DRG neurons.

When F^- was used as an internal anion, an action potential generation was observed even in the presence of TTX in KO neurons (Fig. 8C). This finding indicates that TTX-R/persistent Na^+ current, which could not carry an action potential upstroke when Cl^- was used as an internal anion, may also carry an action potential when the amplitude of TTX-R/persistent Na^+ current was abnormally increased by F^- , although its physiological relevance is uncertain.

Whereas TTX-R/persistent Na^+ current mediated by $Nav1.9$ is actually "persistent" at lower activation voltages (e.g., -60 and -50 mV in Fig. 1C-1), time course of the current becomes considerably fast at higher activation voltages (e.g., voltages positive to -10 mV in Fig. 1C-1). In addition, the time course of the current recorded with F^- as an internal anion is much faster than that recorded with Cl^- as an internal anion when compared at the identical activation voltage, since both the m_∞ and h_∞ curves recorded with F^- as an internal anion were shifted in the negative direction by about 30 mV [25]. Therefore, it is not unlikely that TTX-R/persistent Na^+ current directly mediates an action potential generation in recordings with F^- as an internal anion. The possibility that the TTX-resistant action potential in KO neurons was mediated by the third type of TTX-resistant Na channel, $Nav1.5$, may be excluded, since the TTX-resistant action potential was observed only when F^- was used as an internal anion.

It has been described that internal F^- can activate G protein-mediated mechanisms [11,22,37,42]. Indeed, the amplitude of TTX-R/persistent Na^+ current mediated by $Nav1.9$ was shown to be drastically increased by GTP and its non-hydrolysable analogue GTP- γ -S [3]. In addition, it has been reported that the current mediated by $Nav1.9$ is upregulated by PGE_2 via G-protein activation [32]. Moreover, F^- inhibits activities of a variety of protein phosphatases [28]. Since

biophysical properties of Na⁺ channels are modulated by phosphorylation [8], there is a possibility that F⁻ may affect Nav1.9 through phosphorylation. These reports indicate that F⁻ may affect multiple cellular mechanisms regulating signal transduction. If a similar change in signal transduction took place under some abnormal cellular condition, resultant upregulation of Nav1.9 might significantly affect the electrogenesis of action potential in small DRG neurons.

In conclusion, multiple types of voltage-gated Na⁺ currents could be categorized in small DRG neurons, on the basis of their differential gating kinetics and sensitivity to TTX. One limitation of the study is that the normal site of action potential initiation in sensory neuron is not the cell body. Nevertheless, our results will provide a basis for qualitative interaction between Na⁺ currents in small DRG neurons. Recordings of these Na⁺ currents concurrent with actual membrane potential changes occurring in the same neuron enabled us to study functional contribution of each type of Na⁺ current to the action potential electrogenesis in small DRG neurons. We confirmed that action potentials in DRG neurons are generated and regulated with a combination of multiple types of Na⁺ currents. Such a mechanism, unique to DRG neurons that express heterogeneous TTX-R Na⁺ currents, may play a key role in the processing of sensory information including pain, giving rise to complex patterns of signal encoding in the primary sensory pathway that conduct a variety of sensory modalities.

REFERENCES

1. Akopian AN, Sivilotti L, Wood JN (1996) A tetrodotoxin-resistant voltage-gated sodium channel expressed by sensory neurones. *Nature* 379: 257-262
2. Akopian AN, Souslova V, England S, Okuse K, Ogata N, Ure J, Smith A, Kerr BJ, McMahon SB, Boyce H, Hill R, Stanfa LC, Dickerson AH, Wood JN (1999) The tetrodotoxin-resistant sodium channel SNS has a specialized function in pain pathways. *Nature Neurosci* 2: 541-548
3. Baker MD, Chandra SY, Ding Y, Waxman SG, Wood JN (2003) GTP-induced tetrodotoxin-resistant Na⁺ current regulates excitability in mouse and rat small diameter sensory neurones. *J Physiol (Lond.)* 548: 373-382
4. Benn SC, Costigan M, Tate S, Fitzgerald M, Woolf CJ (2001) Developmental expression of the TTX-resistant voltage-gated sodium channels Nav1.8 (SNS) and Nav1.9 (SNS2) in primary sensory neurons. *J Neurosci* 21: 6077-6085
5. Black JA, Cummins TR, Plumpton C, Chen YH, Hormuzdiar W, Clare JJ, Waxman SG (1999) Upregulation of a silent sodium channel after peripheral, but not central, nerve injury in DRG neurons. *J Neurophysiol* 82:2776–2785
6. Brock JA, McLachlan EM, Belmonte C (1998) Tetrodotoxin-resistant impulses in single nociceptor nerve terminals in guinea-pig cornea. *J Physiol (Lond.)* 512: 211-217
7. Caffrey JM, Eng DL, Black JA, Waxman SG, Kocsis JD (1992) Three types of sodium channels in adult rat dorsal root ganglion neurons. *Brain Res* 592: 283-297
8. Cantrell AR, Catterall WA (2001) Neuromodulation of Na⁺ channels: an unexpected form of cellular plasticity. *Nat Rev Neurosci* 2: 397-407

9. Carl YS, Cummins TR, Waxman SG (2003) GTP γ s increase Na_v1.8 current in small-diameter dorsal root ganglia neurons. *Exp Brain Res* 152: 415-419.
10. Catterall WA (1992) Cellular and molecular biology of voltage-gated sodium channels. *Physiol Rev* 72: S15-48
11. Chen Y, Penington NJ (2000) Competition between internal AlF₄⁻ and receptor-mediated stimulation of dorsal raphe neuron G-proteins coupled to calcium current inhibition. *J Neurophysiol* 83: 1273-1282
12. Coste B, Osorio N, Padilla O, Crest M, Delmas P (2004) Gating and modulation of presumptive Na_v1.9 channels in enteric and spinal sensory neurons. *Mol Cell Neurosci* 26: 123-134
13. Cummins TR, Waxman SG (1997) Downregulation of tetrodotoxin-resistant sodium currents and upregulation of a rapidly repriming tetrodotoxin-sensitive sodium current in small spinal sensory neurons after nerve injury. *J Neurosci* 17: 3503-3514
14. Cummins TR, Dib-Hajj SD, Black JA, Akopian AN, Wood JN, Waxman SG (1999) A novel persistent tetrodotoxin-resistant sodium current in SNS-null and wild-type small primary sensory neurons. *J Neurosci* 19: 1-6
15. Dib-Hajj SD, Tyrrell L, Black JA, Waxman SG (1998) NaN, a novel voltage-gated Na channel, is expressed preferentially in peripheral sensory neurons and down-regulated after axotomy. *Proc Natl Acad Sci USA* 95: 8963-8968
16. Dib-Hajj SD, Tyrell L, Escayg A, Wood PM, Meisler MH, Waxman SG (1999) Coding sequence, genomic organization, and conserved chromosomal localization of the mouse gene *Scn11a* encoding the sodium channel NaN. *Genomics* 59: 309-318

17. Elliot AA, Elliot JR (1993) Characterization of TTX-sensitive and TTX-resistant sodium currents in small cells from adult rat dorsal root ganglia. *J Physiol (Lond.)* 463: 39-56
18. Goldin AL (2001) Resurgence of sodium channel research. *Annu Rev Physiol* 63: 871-894
19. Gruß M, Henrich M, König P, Hempelmann G, Vogel W, Scholz A (2001) Ethanol reduces excitability in a subgroup of primary sensory neurons by activation of BK_{Ca} channels. *Eur J Neurosci* 14: 1246-1256
20. Herzog RI, Cummins TR, Waxman SG (2001) Persistent TTX-resistant Na⁺ current affects resting potential and response to depolarization in stimulated spinal sensory neurons. *J Neurophysiol* 86: 1351-1364
21. Jeftinija S (1994) The role of tetrodotoxin-resistant sodium channels of small primary afferent fibers. *Brain Res* 639: 125-134
22. Kuryshev YA, Naumov AP, Avdonin PV, Mozhayeva GN (1993) Evidence for involvement of a GTP-binding protein in activation of Ca²⁺ influx by epidermal growth factor in A431 cells: effects of fluoride and bacterial toxins. *Cell Signal* 5: 555-64
23. Lee GY, Shin YK, Lee CS, Song J-H (2002) Effects of arachidonic acid on sodium currents in rat dorsal root ganglion neurons. *Brain Res* 950: 95-102
24. Lindia JA, Kohler MG, Martin WJ, Abbadie C (2005) Relationship between sodium channel Nav1.3 expression and neuropathic pain behavior in rats. *Pain* 117: 145-153
25. Maruyama H, Yamamoto M, Matsutomi T, Zheng T, Nakata Y, Wood JN, Ogata N (2004) Electrophysiological characterization of the tetrodotoxin-resistant Na⁺ channel, Nav1.9, in mouse dorsal root ganglion neurons.

Pflugers Arch 449: 76-87

26. Ogata N, Tatebayashi H (1992) Slow inactivation of tetrodotoxin-insensitive Na channels in neurons of rat dorsal root ganglia. *J Membr Biol* 129: 71-80
27. Ogata N, Tatebayashi H (1993) Kinetic analysis of two types of Na⁺ channels in rat dorsal root ganglia. *J Physiol (Lond.)* 466: 9-37
28. Pinkse MWH, Merckx M, Averill BA (1999) Fluoride inhibition of bovine spleen purple acid phosphatase: characterization of a ternary enzyme-phosphate-fluoride complex as a model for the active enzyme-substrate-hydroxide complex. *Biochemistry* 38: 9926-9936
29. Qu Y, Curtis R, Lawson D, Gilbride K, Ge P, DiStefano PS, Silos-Santiago I, Catterall WA, Scheuer T (2001) Differential modulation of sodium channel gating and persistent sodium currents by the β 1, β 2, and β 3 subunits. *Mol Cell Neurosci* 18: 570-580
30. Renganathan M, Cummins TR, Waxman SG (2001) Contribution of Nav1.8 sodium channels to action potential electrogenesis in DRG neurons. *J Neurophysiol* 86: 629-640
31. Rugiero F, Mistry M, Sage D, Black JA, Waxman SG, Crest M, Clerc N, Delmas P, Gola M (2003) Selective expression of a persistent tetrodotoxin-resistant Na⁺ current and Nav1.9 subunit in myenteric sensory neurons. *J Neurosci* 23: 2715-2725
32. Rush AM, Waxman SG (2004) PGE₂ increases the tetrodotoxin-resistant Nav1.9 sodium current in mouse DRG neurons via G-proteins. *Brain Res* 1023: 264-271
33. Rush AM, Brau ME, Elliot AR, Elliot JR (1998) Electrophysiological properties of sodium current subtypes in small cells from adult rat dorsal root

- ganglia. *J Physiol (Lond.)* 511: 771-789
34. Sangameswaran L, Delgado SG, Fish LM, Koch BD, Jakeman, Stewart GR, Sze P, Hunter JC, Eglen RM, Herman, RC (1996) Structure and function of a novel voltage-gated, tetrodotoxin-resistant sodium channel specific to sensory neurons. *J Biol Chem* 271: 5953-5956
 35. Schild JH, Kunze DL (1997) Experimental and modeling study of Na⁺ current heterogeneity in rat nodes neurons and its impact on neuronal discharge. *J Neurophysiol* 78: 3198-3209
 36. Song JH, Nagata K, Huang CS, Yeh JZ, Narahashi T (1996) Differential block of two types of sodium channels by anticonvulsants. *Neuroreport* 25: 3031-3036
 37. Sternweis PC, Gilman AG (1982) Aluminum: A requirement for activation of the regulatory component of adenylate cyclase by fluoride. *Proc Natl Acad Sci USA* 79: 4888-4891
 38. Strassman AM, Raymond SA (1999) Electrophysiological evidence for tetrodotoxin-resistant sodium channels in slowly conducting dural sensory fibers. *J Neurophysiol* 81: 413-424
 39. Vijayaragavan K, Boutjdir M, Chahine M (2004) Modulation of Nav1.7 and Nav1.8 peripheral nerve sodium channels by protein kinase A and protein kinase C. *J Neurophysiol* 91: 1556-1569
 40. Vijayaragavan K, Powell AJ, Kinghorn IJ, Chahine M (2004) Role of auxiliary β_1 -, β_2 -, and β_3 -subunits and their interaction with Nav1.8 voltage-gated sodium channel. *Biochem and Biophys Res Commu* 319: 531-540.
 41. Waxman SG, Kocsis JD, Black JA (1994) Type III sodium channel mRNA is expressed in embryonic but not adult spinal sensory neurons, and is

reexpressed following axotomy. *J Neurophysiol* 72:466–471

42. Yatani A, Brown AM (1991) Mechanism of fluoride activation of G protein-gated muscarinic atrial K⁺ channels. *J Biol Chem* 266: 22872-22877
43. Zhang J-M, Song X-J, LaMotte RH (1999) Enhanced excitability of sensory neurons in rats with cutaneous hyperalgesia produced by chronic compression of the dorsal root ganglion. *J Neurophysiol* 82: 3359-3366

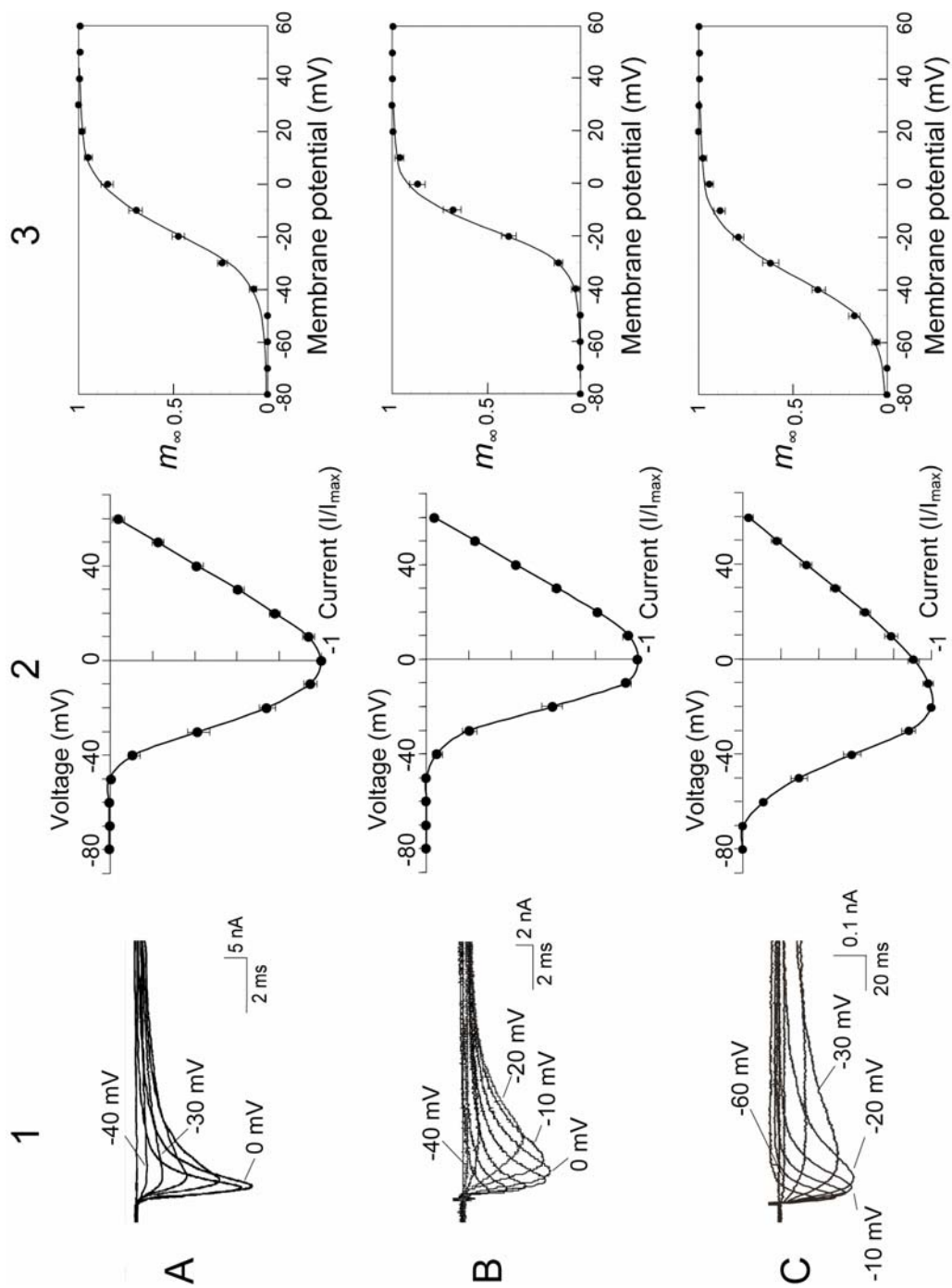


Figure 1. Characterization of Na^+ currents recorded in small DRG neurons.

A, TTX-S/fast Na^+ current. A-1, a family of superimposed TTX-S/fast Na^+ currents evoked by a 200 ms test pulse (V_T) between -80 mV and +60 mV in 10 mV step from a holding

potential (V_H) of -80 mV. The recording was performed in the neuron in which the persistent Na^+ current mediated by $Na_v1.9$ [25] was not detectable. For clarify, Na^+ current evoked by V_T of -40 to +10 mV are shown. The numerals attached to traces indicate the potential of V_T in this and subsequent figures. A-2, the I-V curve for TTX-S/fast Na^+ current ($n = 14$). The current amplitude (I) was normalized to the peak amplitude (I_{max}) for each neuron tested in this and subsequent figures. A-3, the m_∞ curve for TTX-S/fast Na^+ current. The values were plotted against the test pulse potential. Lines were drawn by fitting a Boltzmann function to the means in this and subsequent figures. Although TTX-S/fast Na^+ current was shown using recordings from $Na_v1.8$ knock-out (KO) neurons in this figure, much the same data were also obtained from wild-type (WT) DRG neurons. B, TTX-R/slow Na^+ current recorded in small neurons from WT DRGs. B-1, a family of superimposed TTX-R/slow Na^+ currents evoked by V_T of -40 to +40 mV from V_H of -80 mV. B-2, the I-V curve for TTX-R/slow Na^+ current ($n = 16$). B-3, the m_∞ curve for TTX-R/slow Na^+ current. C, TTX-R/persistent Na^+ current recorded in small neurons from KO DRGs that enabled us to record this TTX-R Na^+ current in isolation. C-1, a family of superimposed TTX-R/persistent Na^+ currents evoked by V_T of -60 to +40 mV from V_H of -80 mV. C-2, the I-V curve of TTX-R/persistent Na^+ current ($n = 18$). C-3, the m_∞ curve of TTX-R/persistent Na^+ current.

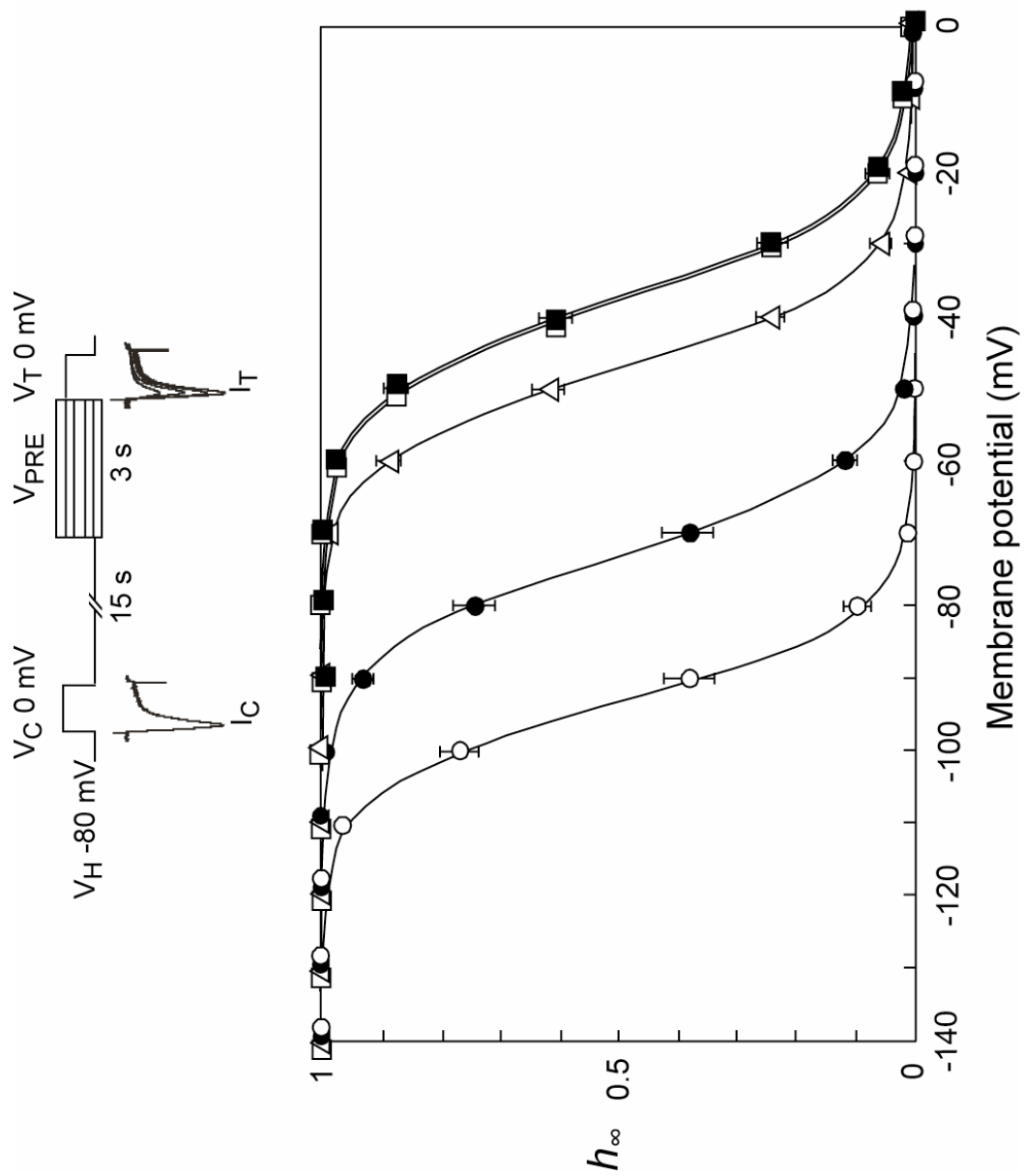


Figure 2. The h_{∞} curves of Na^+ currents in small DRG neurons.

Inset illustrates pulse protocol. Two identical step pulse to 0 mV for 200 ms were applied 15 s prior (V_C) and immediately subsequent (V_T) to the conditioning prepulse (V_{PRE}) of -140

to 0 mV from V_H of -80 mV. The duration of V_{PRE} was 3 s throughout the experiment. The peak amplitude of the current evoked by V_T (I_T) was divided by the peak amplitude obtained with V_C (I_C). The ratio (I_T/I_C) was normalized and plotted against V_{PRE} . The measurement of the h_∞ curve for TTX-R/persistent Na^+ current in WT neurons was performed using V_C and V_T to -20 mV, and amplitudes of I_C and I_T were measured at 100 ms after the beginning of the depolarization. This modification enabled us to obtain the h_∞ curve for TTX-R/persistent Na^+ current in WT neurons, because concurrent TTX-R/slow Na^+ current was already inactivated at 100 ms after the beginning of the depolarization to -20 mV. Open circles, TTX-S/fast Na^+ current in WT neurons ($n = 10$); filled circles, TTX-S/fast Na^+ current in KO neurons ($n = 8$); triangles, TTX-R/slow Na^+ current in WT neurons ($n = 10$); open squares, TTX-R/persistent Na^+ current in WT neurons ($n = 9$); filled squares, TTX-R/persistent Na^+ current in KO neurons ($n = 9$). Error bars for open squares were not shown for clarity. Lines were drawn by fitting a Boltzmann function to the means.

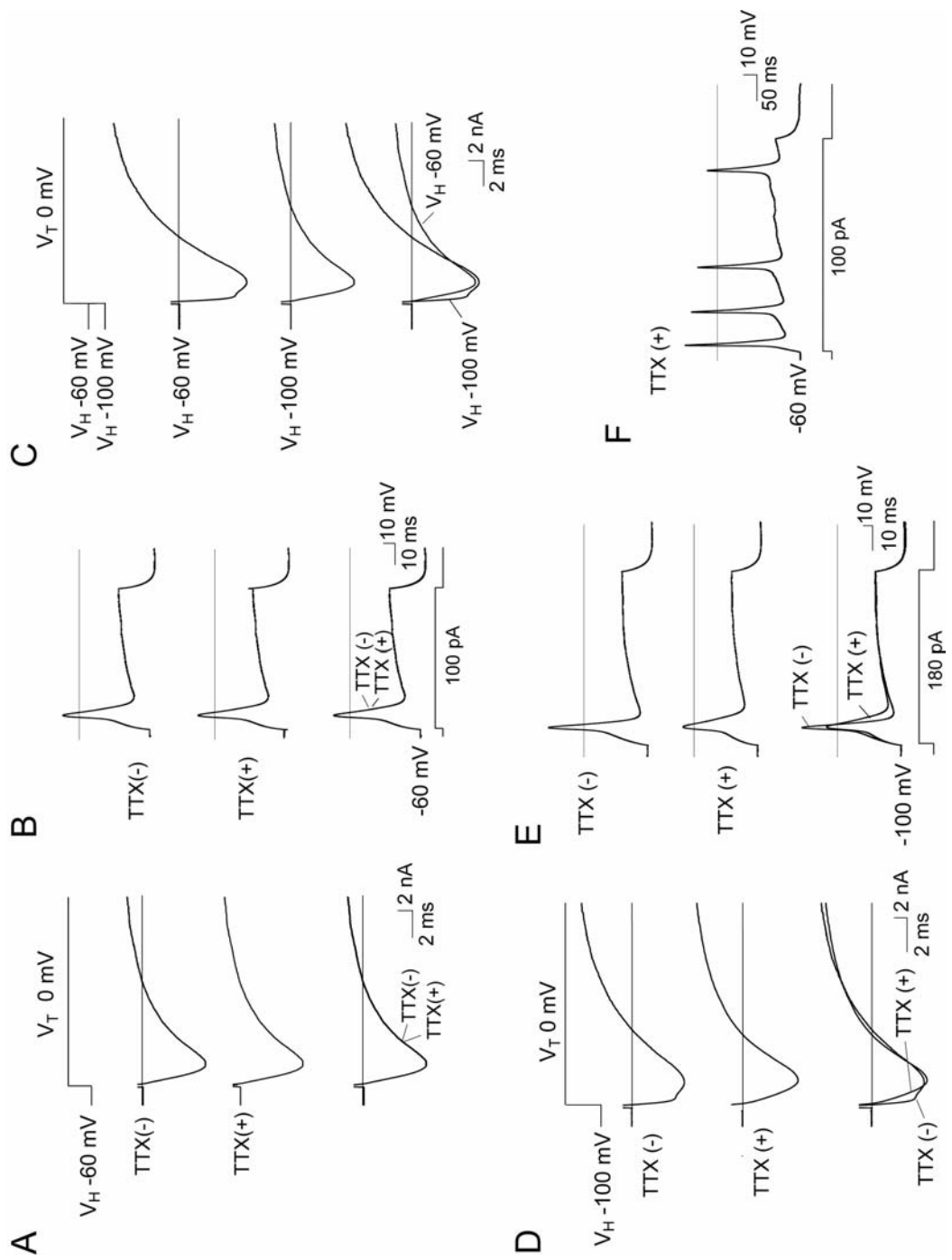


Figure 3. The relationship between Na^+ currents and action potential generation in small neurons from WT DRGs.

Voltage-clamp (A, C and D) and current-clamp (B and E) recordings in the same neuron. A,

the current was evoked by V_T to 0 mV from V_H of -60 mV in the absence or presence of 200 nM TTX. *B*, action potential generated by a 100 pA depolarizing current injection from a membrane potential of -60 mV in the absence or presence of 200 nM TTX. *C*, Na^+ current was evoked by V_T to 0 mV from V_H of -60 mV or -100 mV in the absence of TTX. *D*, the current was evoked by V_T to 0 mV from V_H of -100 mV in the absence or presence of 200 nM TTX. *E*, action potential generated by a 80 pA depolarizing current injection from a membrane potential of -100 mV in the absence or presence of 200 nM TTX. *F*, repetitive firing of action potentials obtained by a 100 pA current injection from a membrane potential of -60 mV in WT small DRG neurons.

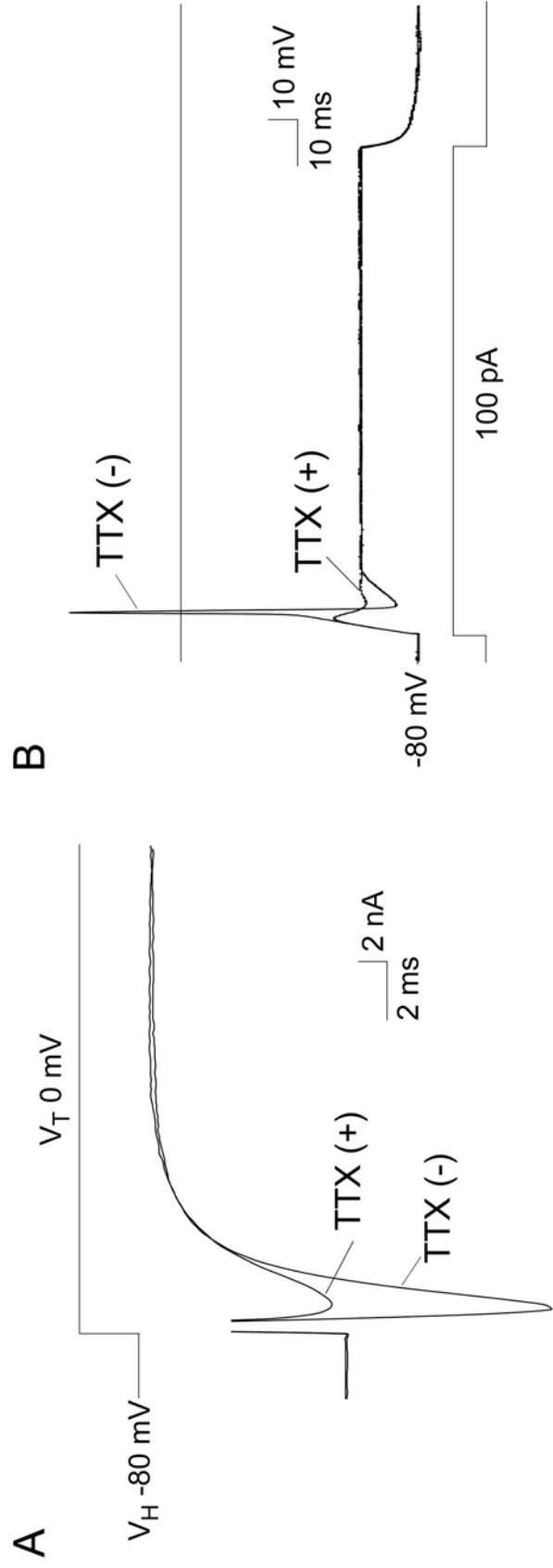


Figure 4. The relationship between Na⁺ currents and action potential generation in small neurons from KO DRGs.

Voltage-clamp (*A*) and current-clamp (*B*) recordings in the same neuron. *A*, the current was evoked by V_T to 0 mV from V_H of -80 mV in the absence or presence of 200 nM TTX. *B*, a potential change in response to a 100 pA depolarizing current injection from a membrane potential of -60 mV in the absence or presence of 200 nM TTX.

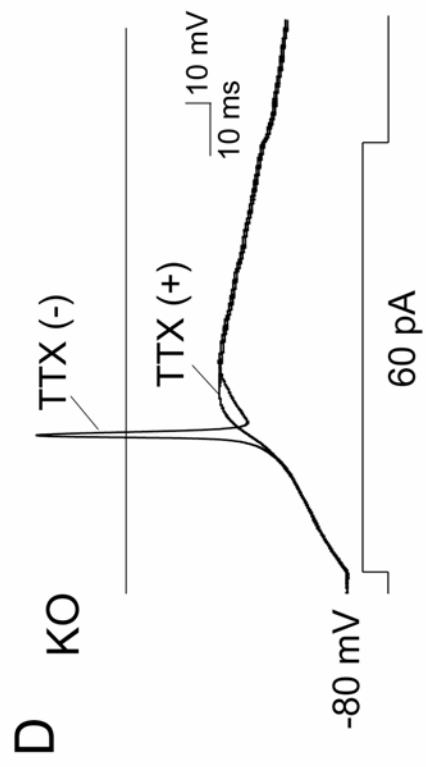
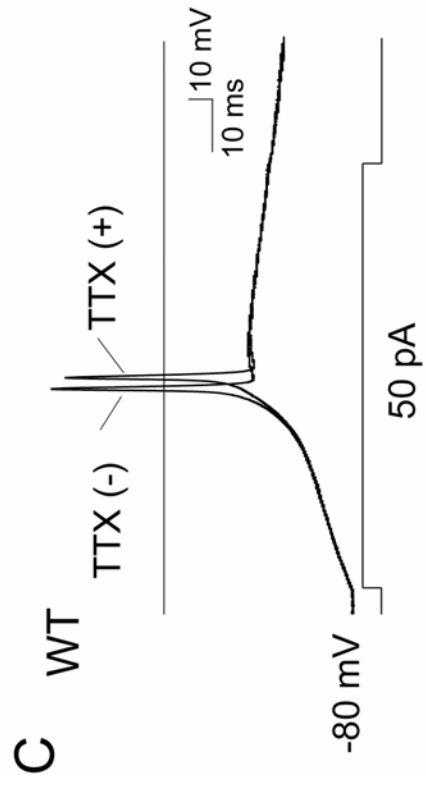
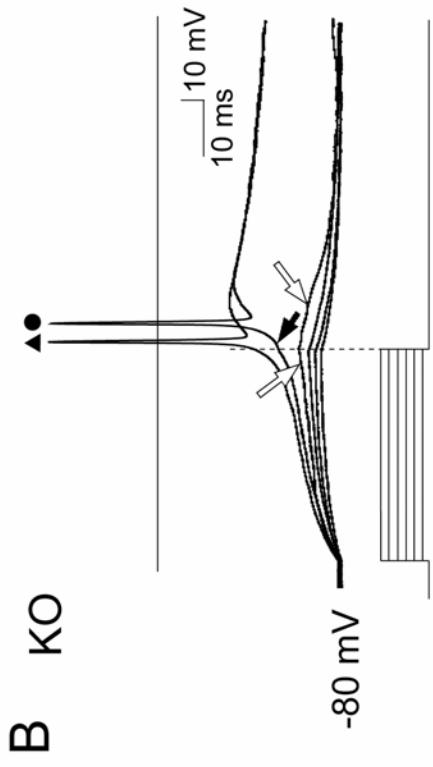
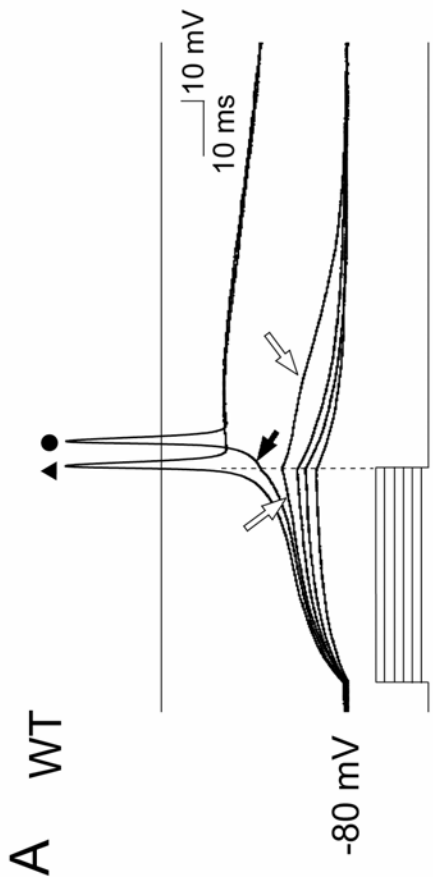


Figure 5. Action potentials induced by the sustained membrane depolarization in small DRG neurons.

A and *B*, families of superimposed membrane potential change evoked by a series of 30 ms depolarizing current injections between 10 and 60 pA in 10 pA step from -80 mV in WT (*A*) and KO (*B*) neurons (for explanation, see text). *C* and *D*, membrane potential changes in response to 50 pA (*C*) or 60 pA (*D*) depolarizing current injections from -80 mV in WT (*C*) or KO (*D*) neurons in the absence or presence of 200 nM TTX. Explanation for symbols, see text.

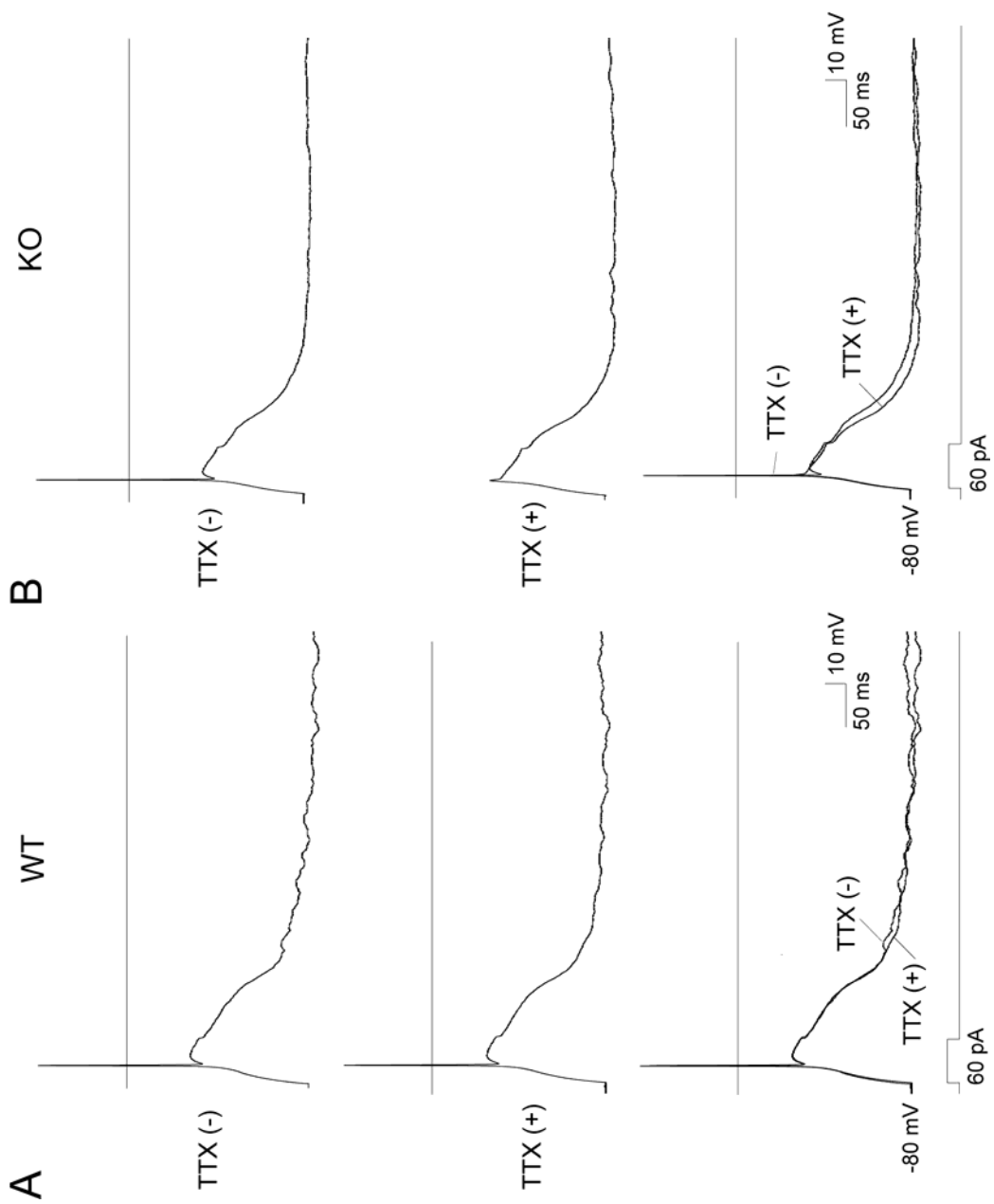


Figure 6. The time course of the sustained membrane depolarization.

The time course of the sustained membrane depolarization was observed by extending the total duration of the trace to 500 ms (*A*, WT, *B*, KO). Membrane potential changes in response to 60 pA depolarizing current injections from -80 mV in the absence or presence of 200 nM TTX. Action potential generation was observed in the presence of TTX in *A* but not in *B*.

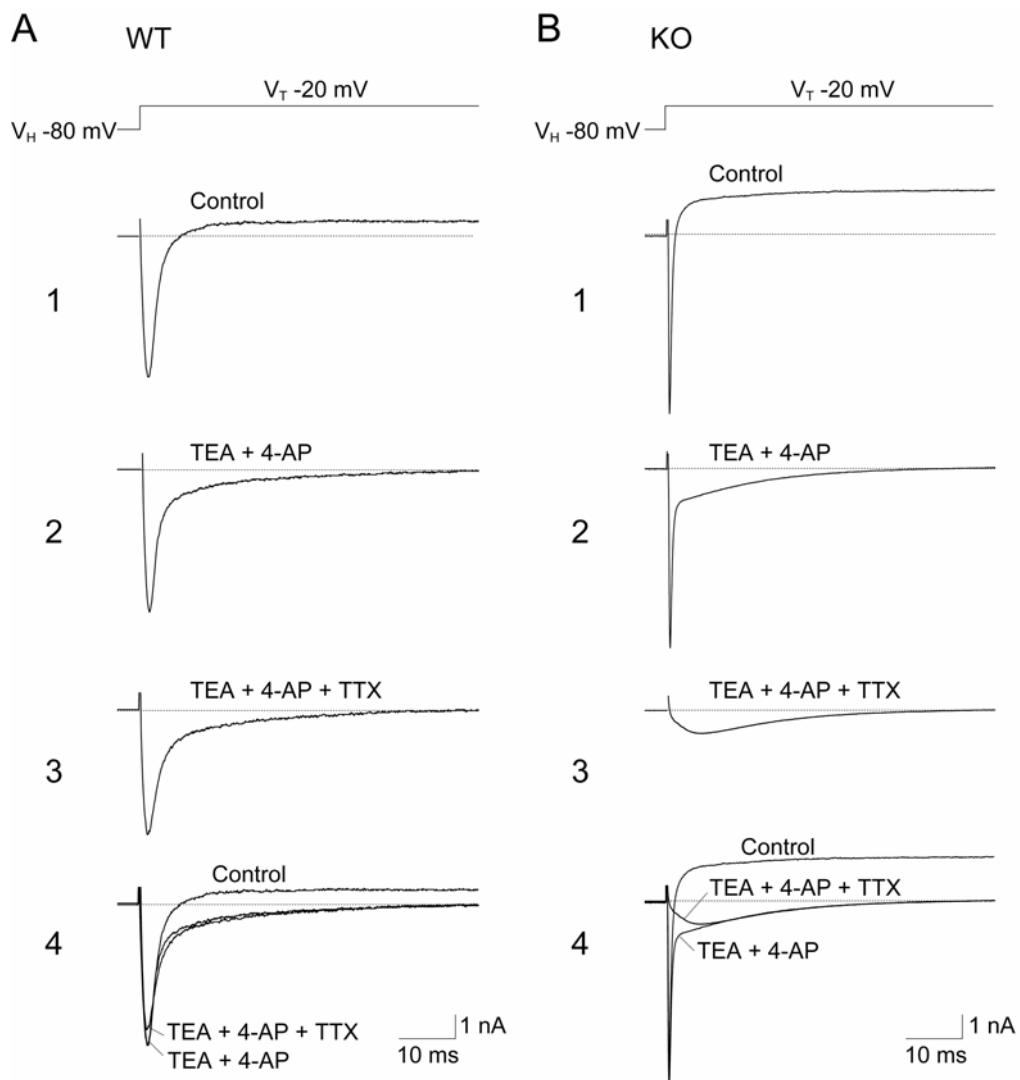


Figure 7. The TTX-R persistent inward component identified in small DRG neurons that showed the sustained membrane depolarization.

Na⁺ currents were evoked by V_T to -20 mV from V_H of -80 mV in neurons from WT (A) and KO (B) DRGs. Traces recorded in the absence of K⁺ channel blockers and TTX (traces 1: control), after addition of K⁺ channel blockers (traces 2: TEA + 4-AP), and after addition of both K⁺ channel blockers and 200 nM TTX (traces 3: TEA + 4-AP + TTX) were superimposed (traces 4). The bath solution including K⁺ channel blockers was prepared by replacing a part of NaCl (30 mM) in the bath solution for current-clamp recording (see Materials and methods) with an equimolar amount of TEA-Cl and adding 5 mM 4-AP. To compensate the concentration of Na⁺ reduced in the bath solution including K⁺ channel blockers, 30 mM NaCl in the original bath solution was replaced with an equimolar tetramethylammonium (TMA)-Cl. TMA ions were used as the non-permeant monovalent cation. The increased osmolarity due to an addition of 4-AP was compensated by reducing glucose. All the recordings were made from the same neurons as those shown in Fig. 6.

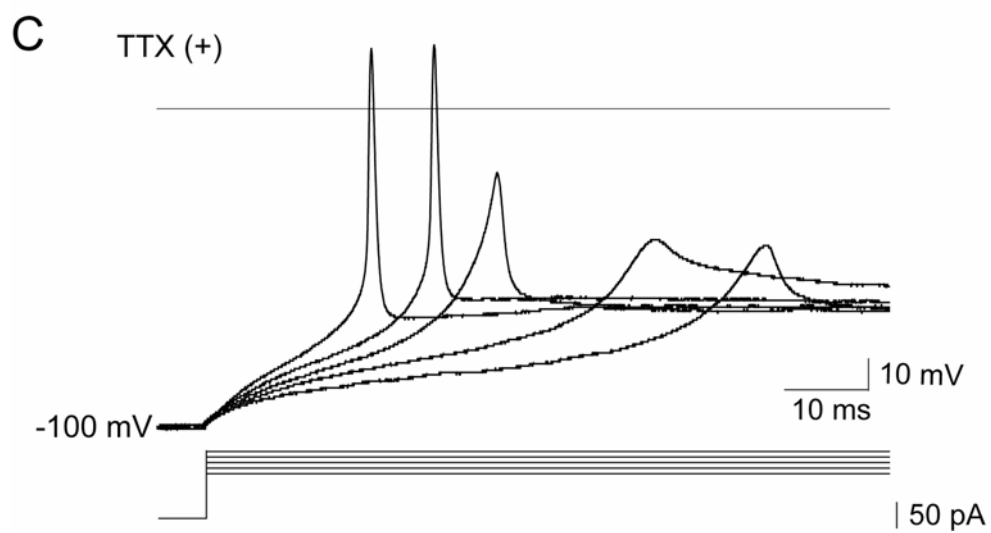
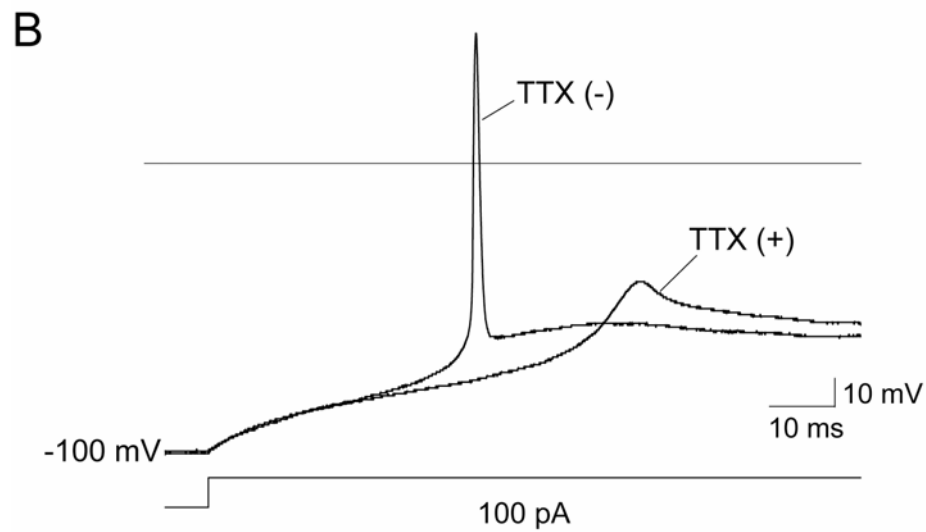
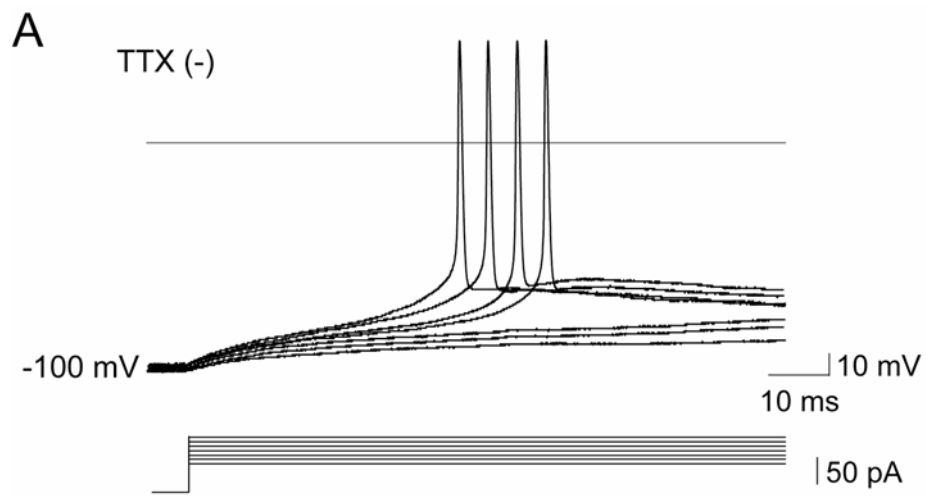


Figure 8. The effect of augmented sustained membrane depolarization on action potential generation in small neurons from KO DRGs.

Current-clamp recordings using F^- as an internal anion. *A*, all-or-none action potentials were evoked by a series of depolarizing current injections between 50 and 110 pA in 10 pA step from a membrane potential of -100 mV. *B*, traces are obtained in response to 80 pA depolarizing current injection from -100 mV in the absence or presence of 200 nM TTX. *C*, a family of superimposed membrane potential change evoked by a series of depolarizing current injections between 80 and 120 pA in 10 pA step from -100 mV in the presence of 200 nM TTX.

Table 1. Activation thresholds and Boltzmann parameters of m_∞ and h_∞ curves for Na⁺ currents in small DRG neurons

Genomic type	TTX-S/fast		TTX-R/slow	TTX-R/persistent		
	WT*	KO	WT	WT	KO	
Activation threshold	-41.6 ± 0.4 (14)**	-41.7 ± 0.3 (12)	-40.3 ± 0.4 (16)	-60.8 ± 0.3 (16)	-61.4 ± 0.4 (18)	
m_∞ curve	$V_{1/2}$	-19.2 ± 1.2 (14)	-20.1 ± 1.4 (12)	-16.4 ± 1.0 (16)	-	-34.8 ± 1.6 (18)
	slope factor	9.2 ± 0.3 (14)	8.9 ± 0.5 (12)	6.9 ± 0.3 (16)	-	9.6 ± 0.2 (18)
h_∞ curve	$V_{1/2}$	-93.2 ± 1.0 (10)	-73.3 ± 1.2 (8)	-47.1 ± 0.8 (10)	-36.8 ± 1.0 (9)	-37.3 ± 0.9 (9)
	slope factor	5.9 ± 0.3 (10)	6.5 ± 0.3 (8)	6.1 ± 0.1 (10)	6.2 ± 0.4 (9)	6.5 ± 0.2 (9)

WT and KO represent wild-type and Na_v1.8 knock-out, respectively.

*Measurements were made in traces obtained by subtracting the currents in the presence of TTX (200 nM) from the currents in the absence of TTX in the same neurone.

**Numerals in parenthesis indicate the number of cells examined

Table 2. Comparison of the current intensity required to evoke an action potential and the threshold for action potential generation in neurons with or without sustained membrane depolarization

Genomic type	Sustained membrane depolarization	Current intensity (pA)	Threshold (mV)	<i>n</i>
Wild-type	+	48.9 ± 2.6	-41.0 ± 0.4	9
	-	137.3 ± 3.3	-40.8 ± 0.5	11
Na _v 1.8-null mutant	+	45.6 ± 2.4	-41.8 ± 0.5	9
	-	133.6 ± 3.4	-42.0 ± 0.4	11

+, present; -, absent; *, significant ($p < 0.01$); n.s., not significant.